Available online at www.sciencedirect.com
SCIENCE DIRECT
Biosensors and Bioelectronics 21 (2006) 1077–1085
BIOSENSORS & BIOELECTRONICS
www.elsevier.com/locate/bios

Application of europium(III) chelate-dyed nanoparticle labels in a competitive atrazine fluoroimmunoassay on an ITO waveguide

C.M. Cummins [a], M.E. Koivunen [b], A. Stephanian [a], S.J. Gee [b], B.D. Hammock [b], I.M. Kennedy [c,*]

[a] *Department of Biomedical Engineering, University of California Davis, Davis, CA 95616, USA*
[b] *Department of Entomology and the UCDavis Cancer Center, University of California Davis, Davis, CA 95616, USA*
[c] *Department of Mechanical and Aeronautical Engineering, University of California, Davis, One Shields Avenue, Davis, CA 95616, USA*

Received 22 January 2005; received in revised form 7 April 2005; accepted 8 April 2005
Available online 28 April 2005

Abstract

We have demonstrated the use of an optical indium tin oxide (ITO) (quartz) waveguide as a new platform for immunosensors with fluorescent europium(III) chelate nanoparticle labels (Seradyn) in a competitive atrazine immunoassay. ITO as a solid surface facilitated the successful use of particulate labels in a competitive assay format. The limit of detection in the new nanoparticle assay was similar to a conventional ELISA. The effect of particle size on bioconjugate binding kinetics was studied using three sizes of bioconjugated particle labels (107, 304, and 396 nm) and a rabbit IgG/anti-IgG system in a 96-well plate. A decrease in particle size resulted in faster binding but did not increase the assay sensitivity. Flux calculations based on the particle diffusivity prove that faster binding of the small particles in this study was primarily due to diffusion kinetics and not necessarily to a higher density of antibodies on the particle surface. The results suggest that ITO could make a good platform for an optical immunosensor using fluorescent nanoparticle labels in a competitive assay format for small molecule detection. However, when used in combination with fluorescent particulate labels, a highly sensitive excitation/detection system needs to be developed to fully utilize the kinetic advantage from small particle size. Different regeneration methods tested in this study showed that repeated washings with 0.1 M glycine–HCl facilitated the reuse of the ITO waveguide.

Keywords: ITO; Immunoassay; Nanoparticles; Lanthanide; Fluorescence; Atrazine

1. Introduction

Immunoassays using antibody/antigen recognition for the detection and quantification of target analytes are applied in both clinical and environmental monitoring, in which herbicides and their metabolites are important target analytes. Compounds such as atrazine or atrazine mercapturate can be detected using an enzyme-linked immunosorbent assay (ELISA) or other immunochemical methods (Karu et al., 1991; Wortberg et al., 1995; Jaeger et al., 1998; Reimer et al., 1998). Atrazine as a member of the triazine herbicide family is of interest because it is one of the most widely used herbicides in the US, and it has been shown to be present in groundwater (Cohen et al., 1986). More importantly, atrazine is classified as a possible human carcinogen by the US Environmental Protection Agency, and it is a known endocrinic disruptor posing a potential health risk to humans (Yu, 2005) as well as to wildlife (Renner, 2002). Current immunochemical methods have been able to detect atrazine at a concentration of 0.1–0.2 ng mL^{-1} (Wortberg et al., 1995; Ciumasu et al., 2005).

Recently, ELISAs have been replaced by more sensitive and faster fluoroimmunoassays (Hall et al., 1999; Schobel et al., 2000). Quantum dots (Chan et al., 2002; Goldman et al., 2002), lanthanide oxide (Feng et al., 2003), and silica nanoparticles doped with lanthanide chelates (Hai et al., 2004; Ye et al., 2004, 2005) or organic dyes (Yang et al.,

* Corresponding author. Tel.: +1 530 752 2796; fax: +1 530 210 8220.
E-mail address: imkennedy@ucdavis.edu (I.M. Kennedy).

0956-5663/$ – see front matter © 2005 Elsevier B.V. All rights reserved.
doi:10.1016/j.bios.2005.04.003

2004) have been proposed as fluorescent markers for immunoassays. However, so far only results from studies using europium chelate-doped, carboxylated polystyrene particles have shown any practical significance (Härmä et al., 2000, 2001; Pelkkikangas et al., 2004). These particles have a major excitation peak at around 333 nm and an emission at 613 nm with a half-life of 0.5 ms. Similarly, europium(III) oxide can be excited at 280, 394 or 466 nm with a long-lifetime emission at 615 nm (Feng et al., 2003). In contrast, most of the widely used organic fluorophores have fluorescence lifetimes in the pico- to nanosecond range. Thus, europium compounds are excellent markers for biological assays, in which a clear differentiation between the signal and background is needed for increased sensitivity. Recently, nanoparticles containing europium have been shown to be effective fluorescent probes in sandwich immunoassays for prostate-specific antigen (PSA)(Härmä et al., 2000, 2001; Soukka et al., 2001b, 2003; Pelkkikangas et al., 2004) or human hepatitis surface antigen (HBsAg) (Hai et al., 2004; Ye et al., 2004) as well as in a competitive immunoassay with magnetic separation for a widely used herbicide, atrazine (Feng et al., 2003).

Bioanalytical assays can be made faster and more sensitive by coupling them to optical immunosensors involving microchannels or waveguides (Rossier et al., 2000; Schuderer et al., 2000; Chabinyc et al., 2001). Usually, immunosensors are based on conventional immunoassay formats. To our knowledge and according to a recent review by Seydack (2005), only a few studies on immunosensors with fluorescent nanoparticle or colloidal gold labels have been published so far (Kubitschko et al., 1997; Schneider et al., 2000a, b). In order to employ nanoparticle labels in biosensor devices, more data are needed on the effect of particle size on the antibody/antigen binding kinetics. So far, there have only been a limited number of studies looking into this important question (Okano et al., 1992; Soukka et al., 2001a). In addition, high non-specific binding of nanoparticle labels on functionalized glass surfaces or poly(dimethylsiloxane) (PDMS) limits their use in microchannels and other flow-through systems and hence, more innovative research is needed to find solid supports for optical immunosensors with nanoparticle labels.

The abundance of surface hydroxyl groups makes electrically conducting indium tin oxide (ITO) surface an attractive platform for immunosensors. Self-assembled monolayers (SAMs) of amphoteric organic molecules form easily on ITO (Yan et al., 2000; Luscombe et al., 2003), and the fact that proteins bind on ITO without any surface modification (Fang et al., 2000, 2003; Hedges et al., 2004) makes it an attractive choice for a solid support in microchannel and waveguide immunoassays with nanoparticle labels. Asanov et al. (1998) and Liron et al. (2002) used ITO successfully for optical waveguide immunosensors. Both studies showed that electrochemical polarization of ITO could be used for the minimization of non-specific binding and the regeneration of optical waveguide surfaces. Similarly, Brusatori et al., 2003 were able to increase the binding of human serum albumin and horse heart cytochrome c on the ITO surface in the presence of an applied potential.

In this work, polystyrene–Eu(III) chelate nanoparticles were used as fluorescent reporters in a competitive fluoroimmunoassay for atrazine. An ITO waveguide was used as a solid support because it offers ideal protein binding properties with minimal non-specific binding of the particle labels. The effect of particle size on the antibody binding kinetics was estimated both mathematically and empirically. Based on these results the assay was optimized using the smallest available (107 nm) particles coupled directly to a monoclonal anti-atrazine antibody, and the sensitivity of the new fluoroimmunoassay was compared with the current 96-well plate ELISA. Furthermore, a range of regeneration methods was evaluated in order to make the use of ITO-based immunosensors less time-consuming and more cost-effective.

2. Experimental

2.1. Antibody coupling to nanoparticles

Europium(III) chelate (tris(naphthyltrifluorobutanedione)) polystyrene nanoparticles (1% solids; 107, 304, and 396 nm) were supplied by Seradyn Inc., Indiana. The particles were attached to goat anti-rabbit IgG (Sigma, St. Louis, MO) or to Protein-A purified monoclonal anti-atrazine antibody (AM7B.2) raised previously by Karu et al. (1991) using a modification of a previously described method (Härmä et al., 2001). The particles were pre-washed on a Nanosep centrifugal filter membrane (300 kDa) with 500 μL 50 mM phosphate buffer, pH 7.0. A particle concentration of 3 μg μL^{-1} in 50 mM phosphate buffer was added to a 200 μL solution of 5 mg *N*-(3-dimethylaminopropyl-*N*-ethylcarbodiimide) (EDAC) and 5 mg *N*-hydroxysulfosuccinimide (Sulfo-NHS) (Sigma, St. Louis, MO) per mL and rotated for 30 min to activate the carboxyl groups on the nanoparticle. The activated particles were washed twice with 50 mM bicarbonate buffer, pH 8.5. A concentration of 1.13 ng mL^{-1} AM7B.2 or 330 μg mL^{-1} of goat anti-rabbit IgG antibody were incubated with the nanoparticles for 2 h in 100 mM bicarbonate buffer, pH 8.3, after which they were washed twice with 50 mM bicarbonate buffer, pH 8.5 suspended in 300 μL of bicarbonate buffer, and stored at 4 °C.

2.2. Competitive assay kinetics in a 96-well plate

In order to determine the optimal particle size for the waveguide assay, the effect of particle size on antibody binding was analyzed using a 96-well plate. Nunc Maxisorp 96-well plates (Nunc, Roskilde, Denmark) were coated overnight at 4 °C with 0.1 mL per well of 3.25 μg mL^{-1} of rabbit IgG (Sigma, St. Louis, MO) in carbonate–bicarbonate buffer (15 mM Na_2CO_3, 35 mM $NaHCO_3$, pH 9.6). The plates were washed three times with PBST (PBS plus 0.05% Tween 20) and blocked for 1 h at room temperature with 0.5%

ovalbumin in PBS. A standard competitive inhibition assay was performed to analyze the effect of particle size on the signal to noise ratio (SNR) and on the IC_{50}, the point of 50% inhibition. Plates coated and blocked with the previously described method were incubated for 1 h with equal volumes of 41.25 μg mL^{-1} of coupled anti-IgG (107, 304, and 396 nm) and IgG (0–130 μg mL^{-1}). The plates were washed three times with PBST and read using the plate reader and the fluorescence intensities were read on a Spectrafluor Plus plate reader (TECAN Systems Inc., CA) with excitation/emission of 330/620 nm.

2.3. Theoretical flux calculation

The effect of particle size on binding kinetics was estimated using Ficks's law (Eq. (1)) for the estimation of the nanoparticle flux to the ITO surface.

$$J = \frac{\sqrt{D}}{\sqrt{\pi t}}C \quad (1)$$

in Eq. (1), C is the particle concentration, t is the time, and the D is the diffusivity. The diffusivity for a spherical particle was determined for each particle size ($2r$ = 107, 304, and 396 nm) using Eq. (2)

$$D = \frac{k_B T}{6\pi\eta r} \quad (2)$$

where k_B is the Boltzman constant, η is the viscosity of water at temperature (T) of 25 °C. Water was chosen as a theoretical medium because the concentration of solutes in solution is very small and does not alter the physical properties of the medium significantly. The flux for each particle size was then used to calculate the amount of particles deposited on a unit ITO surface area over time.

2.4. Antibody surface density quantification

An aliquot (30 μL) of anti-rabbit IgG-polystyrene fluorescent particle (Seradyn Inc., IN) conjugates (107, 304, and 396 nm were incubated separately) were blocked in a 1% BSA solution overnight. Particle conjugates were washed with 50 mM sodium bicarbonate (pH 8.5), after which an aliquot (25 μL) of 560 μg mL^{-1} rabbit IgG coupled to an Alexa Fluor 488 (Molecular Probes, OR) was added, and the suspension was mixed in a rotary mixer for 1 h. Polystyrene particles with no anti-IgG attached were treated the same way and used as controls. The samples were centrifuged at $16.1 \times 10^3 \times g$ for 3 min after which the supernatant was removed and the particles were washed with 500 μL of 50 mM sodium bicarbonate, pH 8.5. The washing process was repeated and the pellet was re-suspended in 100 μL of 50 mM sodium bicarbonate. The fluorescent emission of this suspension was read using an excitation/emission of 485/519 nm on a SpectraMax M2 plate reader (Molecular Devices, Menlo Park, CA). The fluorescence reading from the control particles with no anti-IgG attached was subtracted after which the antibody surface density was determined using a standard curve with known concentrations of IgG-AlexaFluor488 conjugate, and the density was expressed as nanograms of protein per surface area.

2.5. ITO regeneration

The waveguides were cleaned using an RCA method by Donley et al. (2002) (H_2O:H_2O_2:NH_3; 5:1:1, v/v/v; sonicated at 60 °C for 30 min), rinsed with excess deionized water and dried and kept under vacuum at 120 °C. Before use, the resistance of the cleaned waveguides was checked with a hand-held multimeter (GB Instruments, OH) to confirm that the ITO surface was still in place. A concentration of 0.2 mg mL^{-1} of rabbit IgG in 2-(4-morpholino)ethenesulfonic acid (MES), pH 6.0, was incubated for 10 min on the ITO surface after which the waveguides were washed three times with PBST and blocked for 10 min in a solution of 1% BSA in 50 mM sodium bicarbonate, pH 8.5. After washing, 20 μL of 0.22 mg mL^{-1} Alexa Fluor 598-conjugated goat anti-rabbit IgG (Molecular Probes, OR) in 50 mM sodium bicarbonate plus 0.05% Tween 20, pH 8.5 was added on the surface, and incubated for 10 min. After washing with PBST, fluorescence readings were taken at 330 nm/620 nm excitation/emission on a SpectraMax M2 plate reader (Molecular Devices, Menlo Park, CA). The waveguides were then washed three times with one of the following solutions: 0.1 M glycine–HCl; 0.05, 0.16, and 0.45 M NaOH; 10% ethylene glycol; 70% ethanol; 1 × PBS, 5 × PBS, 10 × PBS; and 1 × PBST. After washing, the waveguides were re-incubated with 20 μL of 0.22 mg mL^{-1} AlexaFluor 598 for 10 min as explained above, and another set of fluorescence readings were taken. This cycle was repeated a total of five times.

2.6. Competitive atrazine ELISA on a 96-well plate

A solid phase indirect competitive ELISA was used for measurement of atrazine. Nunc MaxiSorb 96-well plates (Nunc, Roskilde, Denmark) were coated overnight at 4 °C with the coating antigen 2e (synthesized according to Goodrow et al., 1990; 1/18,000 dilution) in a 0.05 M sodium carbonate–bicarbonate buffer (pH 9.6). The following day, the coating antigen was washed off the plate with a phosphate buffered saline solution containing 0.05% Tween 20 (PBST, pH 7.5), and the plate was blocked for 1 h with 0.5% ovalbumin in PBS. After washing, 50 μL of each standard in triplicate was pipetted into each well. The standard curve for atrazine was prepared from the stock standard (1 μg mL^{-1} atrazine in MeOH), and it contained 0–250 ng of atrazine in 1 mL PBST. To each sample well, 50 μL of the anti-atrazine monoclonal antibody (AM7B.2) was added in 1/1000 dilution, and the mixture was incubated at room temperature for 1 h. The sample matrix was washed away leaving only the antibodies bound to the surface coating antigen. Then,

100 μL of the anti-mouse IgG-horseradish peroxidase conjugate (anti-IgG-HRP; 1:5500 dilution; Sigma, St. Louis, MO) was added into each well, and the anti-IgG-HRP was allowed to bind to IgG for 60 min. Unbound anti-IgG-HRP was washed away to leave an amount of HRP enzyme that was inversely proportional to the atrazine concentration in the samples or standards. Finally, a colorless substrate, 1% H_2O_2, and a chromogen, tetramethylbenzidine (TMB) were incubated with the bound enzyme to produce a blue color. A 50 μL aliquot of 2 M H_2SO_4 was added as a stop solution to change the color to a stable yellow. ELISA absorbances at 450 nm were measured with a SpectraMax M2 microplate reader (Molecular Devices, Menlo Park, CA). The software package Softmax (Molecular Devices) was used for fitting the 11-point sigmoidal standard curve based on a four-parameter logistic method of Rodbard (1981).

2.7. Competitive atrazine immunoassay on an ITO waveguide

ITO waveguides (ITO coated quartz, Delta Technologies Limited, MN, 1 cm × 1 cm) were cleaned using the previously described RCA method after which they were incubated with 30 μL of 24 μg mL^{-1} of atrazine coating antigen (2e) for 15 min and then blocked for 30 min with 1% BSA in 50 mM sodium bicarbonate, pH 8.5. A 1:1 ratio of 0.55 μg mL^{-1} of Seradyn 107-nm anti-atrazine-conjugates and aliquots of 0–10,000 ng mL^{-1} of atrazine in bicarbonate buffer were pre-incubated overnight at 4 °C. A 30 μL aliquot of this preincubated mixture was then placed on the waveguides for 30 min. After washing, fluorescence readings were taken at 330 nm/620 nm excitation/emission on a SpectraMax M2 plate reader (Molecular Devices, Menlo Park, CA). Assays were run in three replicates, and the ITO waveguides were washed three times with PBST in-between each incubation step.

3. Results and discussion

3.1. Binding kinetics in a 96-well plate

3.1.1. Experimental

An IgG/anti-IgG kinetic assay first showed that as the particle size increases the emission from the particle conjugates bound to the IgG surface increases, which could be seen as highest emission intensity over time for the biggest particles (Fig. 1). In order to rule out the effect of particle size on the emission intensity, we converted the fluorescence emission intensities into numbers of particles (Fig. 2) by using first a standard curve for intensity versus particle mass and then a mass/number relationship determined earlier by Härmä et al. (2001). This conversion was necessary because the number of particles varied between sizes when masses were kept constant. The slopes of the linear regions (3.1, 0.4, 0.1 particles bound min^{-1} for 107, 304, and 396 nm, respectively) of

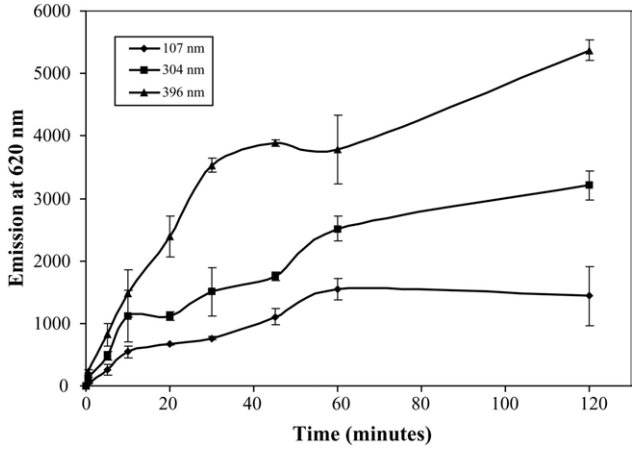

Fig. 1. The fluorescence intensities of 107, 304, and 396-nm particles coupled to goat anti-rabbit IgG and bound on a 96-well plate coated with rabbit IgG. The percentage of CV between three replicate assays was <10%.

the three binding curves in Fig. 2 increased with decreasing particle size, which showed that smaller particles reached equilibrium more quickly. Obviously, this could be caused by faster binding of smaller particles with higher diffusivities. It could also be a direct result of better recognition due to a higher antibody density on the 107-nm particle surface or to more interference of the larger particle labels with the antibody binding reaction.

3.1.2. Theoretical

Our experimental findings support previously reported results with nano-particulate conjugates exhibiting significantly slower reaction rates than standard fluorophores (Koskinen et al., 2004). According to Fick's law (Eqs. (1) and (2)), the increase in particle size results in a decrease in particle flux to the surface. As the particle size increases the particle flux decreases, which in turn decreases the amount of particles transported to the unit surface area over time (Fig. 3). This supports previous findings on bioconjugate kinetics (Hall et al., 1999; Koskinen et al., 2004) and our ex-

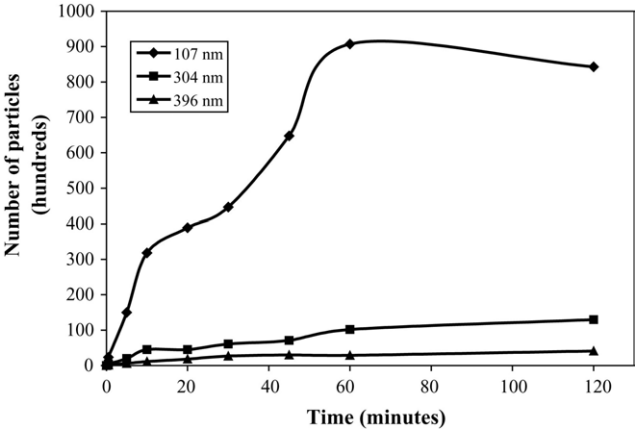

Fig. 2. The effect of particle size on the number of bioconjugated particles bound over time on the surface of a 96-well plate coated with rabbit IgG.

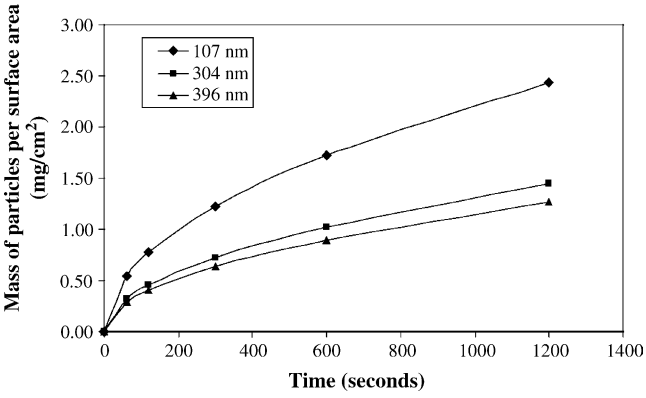

Fig. 3. Mass of particles transported to the ITO surface as a function of time, calculated using a first-order flux approximation for 107, 304 and 396-nm spheres in a semi-infinite solution of water.

perimental observations in this study. However, in order to determine whether the faster binding of small particle conjugates is due to higher density of antibodies on the particle surface or to the fact that smaller particles have higher diffusivity with less steric hindrance, the antibody surface density needed to be examined more in detail.

3.2. Antibody surface density

The measurement of antibodies on different-sized particles revealed that the 107-nm particles had the lowest antibody density on the surface (0.65×10^{-14} ng nm^{-2}), whereas the values for the two larger particles were higher (1.39×10^{-14} and 1.35×10^{-14} ng nm^{-2}, respectively) with no significant differences between the two larger sizes. Even though differences in antibody surface densities were expected, we did not expect any trend among different particle sizes. The result suggests that the fast binding rate of the 107-nm particle conjugate in this case is not due to higher number of antibodies attached to the particle surface, but it is a result of the smaller particle size itself. Soukka et al. (2001a) have already demonstrated that the number of binding sites affects the rate of antibody/antigen binding, and that doubling the number of active sites (a value which is proportional to surface density) on a 107-nm Seradyn particle also doubles the association rate constant and results in a more than three-fold increase in the monovalent affinity constant. However, studies by Kubitschko et al. (1997) and Hall et al. (1999) have indicated that high antibody load can also destabilize the bioconjugates and increase nonspecific binding. Our findings suggest that a higher surface density on a larger particle, i.e., density of active binding sites, does not overrule the negative effect of particle size on the binding rate. In this study, the rate of antibody/antigen binding was primarily regulated by the size of particulate labels and hence, smaller particles seemed to be more suitable for both sandwich and competitive immunoassays.

3.3. Competitive inhibition assay for rabbit IgG in a 96-well plate

A high signal-to-noise ratio (SNR) accompanied by a low IC_{50} value and low background is a requirement for a sensitive competitive ELISA. According to our results from a standard anti-IgG/IgG inhibition assay, particle size affects the SNR (Fig. 4). The 107-nm particle conjugates provided the highest SNR ratio, 10.5, while the 304- and 396-nm particles had an SNR of 2.2 and 2.0, respectively. Similarly, it can be concluded from Fig. 4 that the background noise increases with particle size. For all the particle conjugates tested, the IC_{50} increased with decreasing particle size (IC_{50}: 571, 210, 0.7 ng mL^{-1} for 107, 304, and 396 nm, respectively). It is of interest to note that the 304 and 396-nm particles had a high degree of variability among replicates, which could be explained by a high nonspecific binding of the polystyrene particles on the 96-well plate. A more intense fluorescence is obtained from the big particles, which means that even a small number of nonspecifically bound big particles can contribute to a great variation in the measured signal. High variability among the two larger particle sizes is also demonstrated by the poor fit of the 4-parameter curves: R^2-values were 0.938, 0.839 and 0.890 for 107, 304 and 396-nm particles, respectively.

Based on these results, the 107-nm particle would be most suitable for a competitive immunoassay on a waveguide; it provides the fastest binding with least variability, and based on both a low IC_{50}-value and a high slope of the linear region it also facilitates a quite sensitive assay. According to Fig. 4, higher SNR can be achieved with small particles. However, since the fluorescence intensity also decreases with decreasing particle size, there is a point where a more powerful excitation light source as well as a more sensitive fluorescence detector would be needed for signal recording.

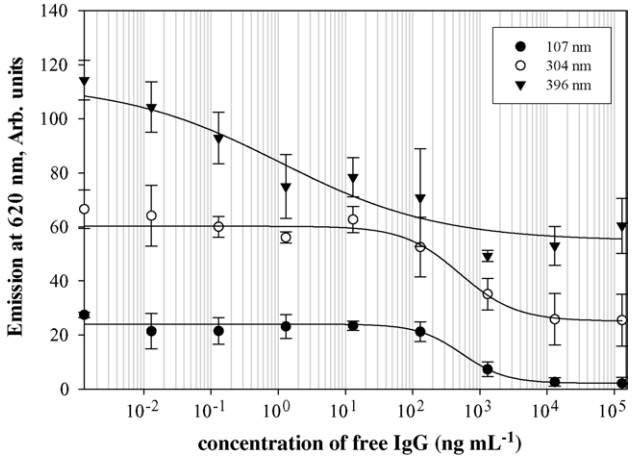

Fig. 4. A 4-parameter curve fitting for the competitive inhibition of goat anti-rabbit IgG coupled to 107, 304, and 396 nm particles with free rabbit IgG.

One of the major limitations for the use of fluorescent nanoparticle labels in immunoassays, and in biosensors in particular, is their tendency to aggregate and bind non-specifically to surfaces (Kubitschko et al., 1997; M.E. Koivunen, personal communication). This phenomenon is due to hydrophobic forces and electrical charges on the particle surfaces, which in some cases can be eliminated by a correct choice of a buffer or by increasing the protein loading on the nanoparticle surface (Soukka et al., 2001a). It should be noted that our attempts to use fluorescent particulate labels in a competitive atrazine immunoassay in a 96-well plate were not successful. Optimization of coating antigen, particle label and blocking agent concentrations as well as changes in incubation time did not help in producing a normal competition-type standard curve. Measurements were hampered by inconsistent readings, most likely caused partly by non-specific binding of the particles to the plate's polystyrene surface.

3.4. Competitive atrazine immunoassay using an ITO Waveguide

A competitive atrazine immunoassay with 107-nm particle conjugate was successfully performed using ITO coated quartz as a solid support, and the standard curve is presented in Fig. 5. The IC_{50} ($\sim$1 ng mL^{-1}) for this 6-point standard curve calculated based on 50% fluorescence inhibition is higher than in a standard 96-well competitive assay (0.143 ng mL^{-1}) shown in Fig. 6, but it still has reasonable sensitivity considering that the current US Environmental Protection Agency's (USEPA) maximal contaminant level for atrazine in drinking water is 3 ng mL^{-1} (ppb). The concentration of atrazine is usually less than 2 ng mL^{-1} in groundwater sources, but has been found at levels as high as 21 ng mL^{-1} in groundwater, 42 ng mL^{-1} in surface waters, and up to 224 ng mL^{-1} in Midwestern streams (Kolpin et al., 1996). However, LOD-values obtained in other published atrazine immunoassays using the same antibody AM7B.2 are lower, in the range of 0.1–0.5 ng mL^{-1} (Wortberg et al., 1995; Feng et al., 2003), which suggests that the sensitivity of this ITO-based competitive atrazine assay could be improved through optimization of the assay conditions. As a comparison, Ciumasu et al. (2005) recently obtained similar sensitivities in their competitive atrazine immunoassays using a different monoclonal antibody in microtiter plates (5 ng mL^{-1}), batch ELISAs (0.3 ng mL^{-1}), and with an immunosensor (0.7 ng mL^{-1}).

According to the literature, fluorescent nanoparticles are excellent candidates for labels in biosensors, because they can increase the assay sensitivity (Härmä et al., 2001; Soukka et al., 2003). Koskinen et al. (2004) reported a decrease in the limit of detection (LOD) by two orders of magnitude using a 75-nm diameter particle label in a sandwich assay in an ArcDia TPX bioaffinity system. Similarly, another study with larger nanoparticles (220 nm) in a heterogeneous sandwich assay for IgG/anti-IgG has shown a 250-fold decrease in LOD when compared to an assay with an organic dye reporter (Hall et al., 1999). However, in our study, no increase in the sensitivity of a competitive atrazine immunoassay using 107-nm fluoresecent europium chelate nanoparticles on an ITO waveguide was found. It should be kept in mind though, that our nanoparticle assay was designed for demonstration and not for sensitive quantitative analytical measurements and hence, it only included six calibrators. One possible reason for lower sensitivity in our assay is a steric hindrance due to particle labels during the competition step (Koskinen et al., 2004), which might affect the binding kinetics. Huhtinen et al. (2004) have recently shown that a streptavidin–biotin link between the antibody and the nanoparticle label increases the flexibility of a bioconjugate system, which can be critical for an enhanced detection of structurally complex analytes. In addition, our experiments were performed without optimization of the antibody density on the particle surface, which also might decrease the assay sensitivity. Future tests should examine if longer incubation times would decrease the IC_{50} and make the assay more sensitive. However, the purpose of this research was to develop a quick immunoassay to be used in a

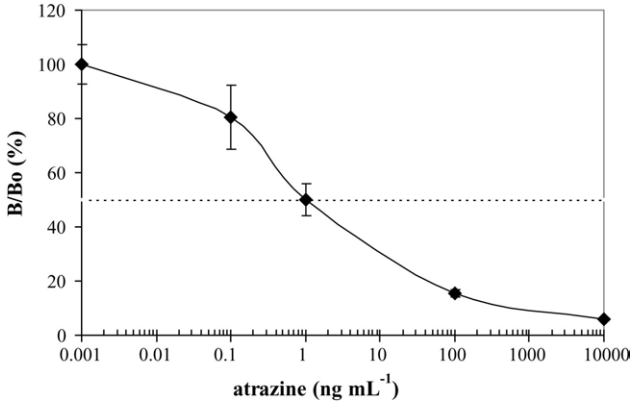

Fig. 5. A standard curve for competitive inhibition assay of atrazine using a monoclonal anti-Atrazine antibody (AM7B.2) coupled to 107-nm Seradyn particles. The assays were performed on an ITO waveguide. B/Bo indicates the relative fluorescence (%). Dotted line indicates the IC_{50}.

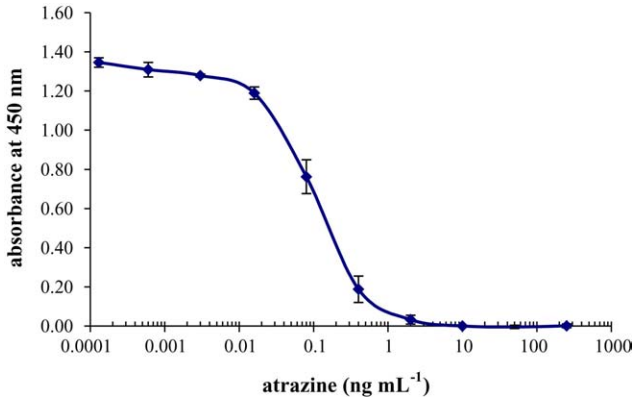

Fig. 6. A 4-parameter curve fitting for the competitive 96-well plate immunoassay for atrazine using a monoclonal antibody (AM7B.2) and a secondary anti-mouse antibody conjugated to a peroxidase enzyme.

biosensor system. Therefore, optimizing the surface density is likely to be a more effective way to increase the sensitivity of this competitive assay. This has already been demonstrated with sandwich immunoassays for PSA (Soukka et al., 2001b), IgG (Hall et al., 1999) and estradiol (Kokko et al., 2004).

Our attempts to develop an atrazine fluoroimmunoassay with nanoparticles in a regular polystyrene 96-well plate were not successful. This may result from the high affinity of particle bioconjugates for atrazine, to the extent that a substantially longer incubation time is required for replacement of the analyte by the surface antigen (atrazine analog). For nanoparticle assays, a long incubation time is generally not desirable because it leads to more particle settling and consequently also to greater degrees of non-specific binding. The fact that we were able to demonstrate concentration-dependent binding of particle conjugates on the ITO waveguide, but not on a polystyrene plate, emphasizes the potential of ITO as a solid support in competitive immunoassays with nanoparticle labels. A more uniform coating of surface antigen on the ITO surface together with less non-specific binding of particles might be the key factors for a competitive immunoassay with nanoparticle labels on an ITO waveguide as demonstrated in this study.

In the future, an increasing number of immunochemical methods for clinical and environmental analysis are going to be adapted to optical immunosensors involving microchannels or waveguides (Van Emon and Gerlach, 1998) which can improve both assay sensitivity and throughput. Continuous-flow immunosensors based on sandwich assays and fluorescence detection have been demonstrated for large molecules (Koch et al., 2000; Eteshola and Leckband, 2001; Hofmann et al., 2002), but the development of fluoroimmunosensors involving competitive assay formats for small molecules, like pesticides, has been hampered by the lack of suitable platforms. Our study on the development of a competitive atrazine fluoroimmunoassay on an ITO surface is a first successful attempt to combine a solid surface with unique chemical and physical properties and fluorescent nanoparticles. Since the sensitivity of a competitive immunoassay is mostly determined by the affinity of the antibody for its antigen (Warsinke et al., 2000), a sensitive biosensor for small molecule competitive assays requires a high-affinity biospecific interaction facilitated by a solid support with good response characteristics and good reproducibility. Based on our results simulating stopped-flow conditions, ITO seems to be applicable as a platform for competitive immunoassays with nanoparticle labels, which could be adapted to optical biosensors involving online flow-through systems on waveguides, microchannels or microchips. Undoubtedly, ITO could also be used in immunosensors involving non-competitive (sandwich) assays, in which diffusion processes are much more important than the affinity of the antibody (Warsinke et al., 2000), and which, by nature, are faster and more sensitive than competitive immunoassays (Jackson and Ekins, 1986).

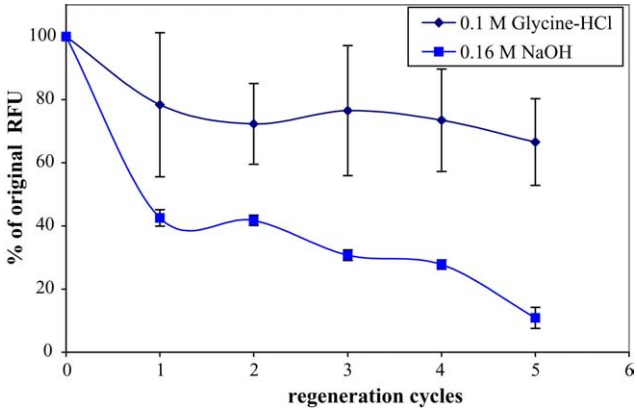

Fig. 7. Fluorescence emission (percentage of original RFU) after sequential regeneration of ITO surface with two different solvents.

3.5. ITO regeneration

In order to facilitate fast and continuous analysis of samples with flow-through immunosensors, the sensor's active surface with bound antigens or antibodies has to be easily regenerated. For most solid supports, treatments with extreme pH, temperature, or chaotropic agents are required to dissociate the antibody–antigen complexes. Regeneration of the ITO surface without stripping off the surface antigen was tested with several solvents generally used in immunoaffinity column regeneration. Of all agents tested, 0.1 M Glycine–HCl and 0.16 M NaOH were most effective (Fig. 7). However, the variation between replicates was extremely high for the 0.1 M Glycine–HCl, which can be explained by the fact that ITO is degraded by acids (Folcher et al., 1997; Donley et al., 2002; Huang et al., 2003). Regeneration with a base, NaOH, was not successful either, resulting in a severe stripping of the surface antigens and a decrease in antibody binding after each regeneration cycle. According to our results, chemical regeneration methods might not offer the best possible means for fast and effective surface regeneration of ITO platforms. Future studies will show whether electrochemical modulation of ITO surfaces demonstrated earlier by several groups (Asanov et al., 1998; Liron et al., 2002; Brusatori and Van Tassel, 2003; Gooding et al., 2004) can be utilized to regulate interaction of nanoparticle bioconjugates and surface antigens allowing for immunosensor regeneration as well as for regulation of non-specific binding.

4. Conclusion

We have demonstrated the use of an indium tin oxide surface as a solid support for a competitive fluoroimmunoassay for an herbicide, atrazine, with europium chelate-dyed polystyrene particle labels. This is the first time fluorescent nanoparticle labels have been successfully used in a competitive immunoassay for a small molecule. The results showed that without further assay optimization the fluores-

cent nanoparticle labels did not increase assay sensitivity compared to the current conventional 96-well plate atrazine ELISA. To decrease the detection limit and to create a highly sensitive atrazine biosensor, more tests are needed to optimize all assay parameters including the antibody density on the particle surface. On the other hand, the novel finding that ITO facilitated the use of nanoparticle labels in a competitive fluoroimmunoassay for a small molecule, atrazine, suggests that it could offer an ideal platform for flow-through fluoroimmunosensors on waveguides, microchannels and chips. Regeneration of activated ITO surface is possible by chemical methods. However, future studies will show whether electrochemical modulation of ITO would help in both assay optimization and biosensor regeneration.

In addition, we were able to show, both empirically and mathematically, that as the size of the europium chelate-dyed polystyrene particles decreases, the time required for binding decreases. While the fluorescence intensity also decreases with decreasing particle size, it seems obvious that in order to facilitate the use of small nanoparticle labels in immunoassays, powerful excitation light sources and sensitive fluorescence detectors are required for signal recording.

Acknowledgments

The authors wish to acknowledge the support of the National Science Foundation, Grant DBI-0102662 and the Superfund Basic Research Program with Grant 5P42ES04699 from the National Institute of Environmental Health Sciences, NIEH.

References

Asanov, A.N., Wilson, W.W., Oldham, P.B., 1998. Regenerable biosensor platform: a total internal reflection fluorescence cell with electrochemical control. Anal. Chem. 70, 1156–1163.

Brusatori, M.A., Van Tassel, P.R., 2003. Biosensing under an applied voltage using optical waveguide lightmode spectroscopy. Biosens. Bioelectron. 18, 1269–1277.

Brusatori, M.A., Tie, Y., Van Tassel, P.R., 2003. Protein adsorption kinetics under an applied electric field: an optical waveguide lightmode spectroscopy study. Langmuir 19, 5089–5097.

Chabinyc, M.L., Chiu, D.T., McDonald, J.C., Stroock, A.D., Christian, J.F., Karger, A.M., Whitesides, G.M., 2001. An integrated fluorescence detection system in poly(dimethylsiloxane) for microfluidic applications. Anal. Chem. 73, 4491–4498.

Chan, W.C.W., Maxwell, D.J., Gao, X., Bailey, R.E., Han, M., Nie, S., 2002. Luminescent quantum dots for multiplexed biological detection and imaging. Curr. Opin. Biotech. 13, 40–46.

Ciumasu, I.M., Kramer, P.M., Weber, C.M., Kolb, G., Tiemann, D., Windisch, S., Frese, I., Kettrup, A.A., 2005. A new, versatile field immunosensor for environmental pollutants. Development and proof of principle with TNT, diuron, and atrazine. Biosens. Bioelectron. 21, 354–364.

Cohen, S.Z., Eiden, C., Lorber, M.N., 1986. Monitoring groundwater for pesticides. In: Proceedings of the ACS Symposium Series 315, pp. 170–196.

Donley, C., Dunphy, D., Paine, D., Carter, C., Nebesny, K., Lee, P., Alloway, D., Armstrong, N.R., 2002. Characterization of indium-tin oxide surfaces using X-ray photoelectron spectroscopy and redox processes of a chemisorbed probe molecule: effects of surface pretreatment conditions. Langmuir 18, 450–457.

Eteshola, E., Leckband, D., 2001. Development and characterization of an ELISA assay in PDMS microfluidic channels. Sens. Actuator B: Chem. 72, 129–133.

Fang, A.P., Ng, H.T., Su, X.D., Li, S.F.Y., 2000. Soft-lithography-mediated submicrometer patterning of self-assembled monolayer of hemoglobin on ITO surfaces. Langmuir 16, 5221–5226.

Fang, A.P., Ng, H.T., Li, S.F.Y., 2003. A high-performance glucose biosensor based on monomolecular layer of glucose oxidase covalently immobilised on indium-tin oxide surface. Biosens. Bioelectron. 19, 43–49.

Feng, J., Shan, G.M., Maquieira, A., Koivunen, M.E., Guo, B., Hammock, B.D., Kennedy, I.M., 2003. Functionalized europium oxide nanoparticles used as a fluorescent label in an immunoassay for atrazine. Anal. Chem. 75, 5282–5286.

Folcher, G., Cachet, H., Froment, M., Bruneaux, J., 1997. Anodic corrosion of indium tin oxide films induced by the elctrochemical oxidation of chlorides. Thin Solid Films 301, 242–248.

Goldman, E.R., Anderson, G.P., Tran, P.T., Mattoussi, H., Charles, P.T., Mauro, J.M., 2002. Conjugation of luminescent quantum dots with antibodies using an engineered adaptor protein to provide new reagents for fluoroimmunoassays. Anal. Chem. 74, 841–847.

Gooding, J.J., Wasiowych, C., Barnett, D., Hibbert, D.B., Barisci, J.N., Wallace, G.G., 2004. Electrochemical modulation of antigen–antibody binding. Biosens. Bioelectron. 20, 260–268.

Goodrow, M.H., Harrison, R.O., Hammock, B.D., 1990. Hapeten synthesis, antibody development, and competitive inhibition enzyme immunoassay for s-triazine herbicides. J. Agric. Food Chem. 38, 990–996.

Hai, X., Tan, M., Wang, G., Ye, Z., Yuan, J., Matsumoto, K., 2004. Preparation and a time-resolved fluoroimmunoassay application of new europium fluorescent nanoparticles. Anal. Sci. 20, 245–246.

Hall, M., Kazakova, I., Yao, Y.M., 1999. High sensitivity immunoassays using particulate fluorescent labels. Anal. Biochem. 272, 165–170.

Hedges, D.H.P., Richardson, D.J., Russell, D.A., 2004. Electrochemical control of protein monolayers at indium tin oxide surfaces for the reagentless optical biosensing of nitric oxide. Langmuir 20, 1901–1908.

Hofmann, O., Voirin, G., Niedermann, P., Manz, A., 2002. Three-dimensional microfluidic confinement for efficient sample delivery to biosensor surfaces. Application to immunoassays on planar optical waveguides. Anal. Chem. 74, 5243–5250.

Huang, C.A., Li, Y.K., Tu, G.C., Wang, W.S., 2003. The electrochemical behavior of tin-doped indium oxide during reduction in 0.3 M hydrochloric acid. Electrochim. Acta 48, 3599–3605.

Huhtinen, P., Soukka, T., Lövgren, T., Härmä, H., 2004. Immunoassay of total prostate-specific antigen using europium(III) nanoparticle labels and streptavidin–biotin technology. J. Immunol. Methods 294, 111–122.

Härmä, H., Soukka, T., Lönnberg, S., Paukkunen, J., Tarkkinen, P., Lövgren, T., 2000. Zeptomole detection sensitivity of prostate-specific antigen in a rapid microtitre plate assay using time-resolved fluorescence. Luminescence 15, 351–355.

Härmä, H., Soukka, T., Lövgren, T., 2001. Europium nanoparticles and time-resolved fluorescence for ultrasensitive detection of prostate-specific antigen. Clin. Chem. 47, 561–568.

Jaeger, L.L., Jones, A.D., Hammock, B.D., 1998. Development of an enzyme-linked immunosorbent assay for atrazine mercapturic acid in human urine. Chem. Res. Toxicol. 11, 342–352.

Jackson, T.M., Ekins, R.P., 1986. Theoretical limitations on immunoassay sensitivity. Current practice and potential advantages of fluorescent Eu3+ chelates as non-radioisotopic tracers. J. Immunol. Methods 87, 13–20.

Karu, A.E., Harrison, R.O., Schmidt, D.J., Clarkson, C.E., Grassman, J., Goodrow, M.H., Lucas, A., Hammock, B.D., Vanemon, J.M., White, R.J., 1991. Monoclonal immunoassay of triazine herbicides—development and implementation. In: Proceedings of the ACS Symposium Series 451, pp. 59–77.

Koch, S., Wolf, H., Danapel, C., Feller, K.A., 2000. Optical flow-cell multichannel immunosensor for the detection of biological warfare agents. Biosens. Bioelectron. 14, 779–784.

Kokko, L., Sandberg, K., Lövgren, T., Soukka, T., 2004. Europium(III) chelate-dyed nanoparticles as donors in a homogeneous proximity-based immunoassay for estradiol. Anal. Chim. Acta 503, 155–162.

Kolpin, D.W., Sneck-Fahrer, D.A., Hallberg, G.R., Libra, R.D., 1996. Temporal trends of selected agricultural chemicals in Iowa's groundwater, 1982–1995: are things getting better? J. Environ. Qual. 26, 1007–1017.

Koskinen, J.O., Vaarno, J., Meltola, N.J., Soini, J.T., Hanninen, P.E., Luotola, J., Waris, M.E., Soini, A.E., 2004. Fluorescent nanoparticles as labels for immunometric assay of c- reactive protein using two-photon excitation assay technology. Anal. Biochem. 328, 210–218.

Kubitschko, S., Spinke, J., Bruckner, T., Pohl, S., Oranth, N., 1997. Sensitivity enhancement of optical immunosensors with nanoparticles. Anal. Biochem. 253, 112–122.

Liron, Z., Tender, L.M., Golden, J.P., Ligler, F.S., 2002. Voltage-induced inhibition of antigen–antibody binding at conducting optical waveguides. Biosens. Bioelectron. 17, 489–494.

Luscombe, C.K., Li, H.W., Huck, W.T.S., Holmes, A.B., 2003. Fluorinated silane self-assembled monolayers as resists for patterning indium tin oxide. Langmuir 19, 5273–5278.

Okano, K., Takahashi, S., Yasuda, K., Tokinaga, D., Imai, K., Koga, M., 1992. Using microparticle labeling and counting for attomole level detection in heterogeneous immunoassay. Anal. Biochem. 202, 120–125.

Pelkkikangas, A.M., Jaakohuhta, S., Lövgren, T., Härmä, H., 2004. Simple, rapid, and sensitive thyroid-stimulating hormone immunoassay using europium(III) nanoparticle label. Anal. Chim. Acta 517, 169–176.

Reimer, G.J., Gee, S.J., Hammock, B.D., 1998. Comparison of a time-resolved fluorescence immunoassay and an enzyme-linked immunosorbent assay for the analysis of atrazine in water. J. Agric. Food Chem. 46, 3353–3358.

Renner, L., 2002. Atrazine linked to endocrine disruption in frogs. Environ. Sci. Technol. 36, 55A–56A.

Rodbard, D., 1981. Ligand Assay. In: Langan, J., Clapp, J.J. (Eds.), Mathematics and Statistics in Ligand Assay. Massin Publishing, New York, pp. 45–99.

Rossier, J.S., Gokulrangan, G., Girault, H.H., Svojanovsky, S., Wilson, G.S., 2000. Characterization of protein adsorption and immunosorption kinetics in photoablated polymer microchannels. Langmuir 16, 8489–8494.

Seydack, M., 2005. Nanoparticle labels in immunosensing using optical detection methods. Biosens. Bioelectron. 20, 2454–2469.

Schneider, B.H., Dickinson, E.L., Vach, M.D., Hoijer, J.V., Howard, L.V., 2000a. Highly sensitive optical chip immunoassays in human serum. Biosens. Bioelectron. 15, 13–22.

Schneider, B.H., Dickinson, E.L., Vach, M.D., Hoijer, J.V., Howard, L.V., 2000b. Optical chip immunoassay of hCG in human whole blood. Biosens. Bioelectron. 15, 597–604.

Schobel, U., Barzen, C., Gauglitz, G., 2000. Immunoanalytical techniques for pesticide monitoring based on fluorescence detection. Fresenius. J. Anal. Chem. 366, 646–658.

Schuderer, J., Akkoyun, A., Brandenburg, A., Bilitewski, U., Wagner, E., 2000. Development of a multichannel fluorescence affinity sensor system. Anal. Chem. 72, 3942–3948.

Soukka, T., Härmä, H., Paukkunen, J., Lövgren, T., 2001a. Utilization of kinetically monovalent binding affinity by immunoassays based on multivalent nanoparticle-antibody bioconjugates. Anal. Chem. 73, 3511.

Soukka, T., Paukkunen, J., Härmä, H., Lönnberg, S., Lindroos, H., Lövgren, T., 2001b. Supersensitive time-resolved immunofluorometric assay of free prostate-specific antigen with nanoparticle label technology. Clin. Chem. 47, 1269–1278.

Soukka, T., Antonen, K., Härmä, H., Pelkkikangas, A.M., Huhtinen, P., Lövgren, T., 2003. Highly sensitive immunoassay of free prostate-specific antigen in serum using europium(III) nanoparticle label technology. Clin. Chim. Acta 328, 45–58.

Van Emon, J.M., Gerlach, C.L., 1998. Expanding the role of environmental immunoassays: Technical capabilities, regulatory issues, and communication vehicles. Anal. Chem. Acta 376, 55–59.

Warsinke, A., Benkert, A., Scheller, F.W., 2000. Electrochemical immunoassays. Fresenius J. Anal. Chem. 366, 622–634.

Wortberg, M., Kreissig, S.B., Jones, G., Rocke, D.M., Hammock, B.D., 1995. An immunoassay for the simultaneous determination of multiple triazine herbicides. Anal. Chim. Acta 304, 339–352.

Yan, C., Zharnikov, M., Golzhauser, A., Grunze, M., 2000. Preparation and characterization of self-assembled monolayers on indium tin oxide. Langmuir 16, 6208–6215.

Yang, W., Zhang, C.G., Qu, H.Y., Yang, H.H., Xu, J.G., 2004. Novel fluorescent silica nanoparticle probe for ultrasensitive immunoassays. Anal. Chim. Acta 503, 163–169.

Ye, Z., Tan, M., Wang, G., Yuan, J., 2004. Novel fluorescent europium chelate-doped silica nanoparticles: preparation, characterization and time-resolved fluorometric application. J. Mater. Chem. 14, 851–856.

Ye, Z., Tan, M., Wang, G., Yuan, J., 2005. Development of functionalized terbium fluorescent nanoparticles for antibody labeling and time-resolved fluoroimmunoassay application. Talanta 65, 206–210.

Yu, M.-H., 2005. Environmental Toxicology. Biological and Health Effects of Pollutants, second ed. CRC Press LLC, Boca Raton, FL, 339 pp.